IRAQI JOURNAL OF MATERIALS
Volume (5) Issue (3) July-September 2026, pp. 133-140
Published and Sponsored by American Quality for Scientific Publishing, Inc. (AQSP)

Mechanical Characteristics of Al-Si Casting Alloys Reinforced with SiC Nanoparticles

Sarah M. Taleb, Basheer H. Hmud*

Department of Physics, College of Science, Thi Qar University, Naseriyah, IRAQ
** Corresponding author email: hammad.humud@gmail.com*

Abstract
In this work, composite materials were prepared from aluminum-silicon (Al-Si) alloy (A356) reinforced with silicon carbide (SiC) nanoparticles with different percentage volumetric contents (from 0 to 5 vol.%) using casting method with mechanical stirring. Results of the transmission and scanning electron microscopy (TEM and SEM) showed inhomogeneous distribution of the SiC nanoparticles as dense clusters at high contents, which caused a degradation in the mechanical properties despite the increasing content of the reinforcing material (SiC nanoparticles). The Brinell hardness, yield strength, and ultimate tensile strength (UTS) were determined and compared to the unreinforced fundamental sample (0 vol.% SiC). The enhancement in these properties is attributed to the grain crystallinity with minimum size of 16 µm as well as strengthening mechanisms, whereas the porosity and particle clusters caused the mechanical properties to degrade when the optimum content of the reinforcing material (SiC nanoparticles) is exceeded as the fracture mode converts from completely ductile to a mix of ductile-brittle with dominant brittleness.

***Keywords*:** Al-Si alloy; Silicon carbide; Nanoparticles; Mechanical properties; Casting
Received: April 2026; **Revised:** May 2026; **Accepted:** June 2026; **Published:** July 2026

1. Introduction

The Al-Si alloys are among the most metallic materials used in the applications of mechanical engineering, space and automobile industry due to their unique characteristics including low density, excellent casting capability, good corrosion resistance, and relatively high thermal conductivity [1-3]. Despite these advantages, the performance of these alloys under the conditions of thermal-mechanical stresses is limited due to some original structural defects such as rough and needle-like silicon phase that acts as stress concentrating sites and hence reduces toughness and fracture resistance [4-6]. Therefore, tends to develop metallic-matrix composites (MMCs) in order to enhance the mechanical properties of these alloys throughout the incorporation of ceramic reinforcing materials homogeneously distributed within the matrix (alloy) [7-9]. This may allow to achieve a balance between lightweight and high strength, which is a major requirement in modern engineering design [10-12].

In this context, silicon carbide (SiC) nanoparticles have gained drastic interest as an ideal selection to reinforce the Al-Si alloys due to their super-hardness, high elastic modulus, thermal stability, and relatively low cost when compared to other types of ceramic nanomaterials [13-16]. Contradicting the micro particles, nanoparticles provide an ultrahigh surface-to-volume ratio that enhances the interaction between the reinforcing particles and the metallic matrix as well as increase their ability to hinder the movement of dislocations and limit the grain growth during resolidification process [17-19]. The largest challenge is represented by achieving homogeneous distribution of these nanoparticles within the matrix, avoid the cluster phenomenon that leads to form pores and weak regions, and hence necessarily control the undesired chemical reactions at the interfaces that may result brittle phases such as aluminum carbide and silicide [20-22].

Accordingly, the aim of this study is to analyze and characterize the mechanical properties of Al-Si alloys prepared by mechanical stirring casting and reinforced with SiC nanoparticles at different volumetric contents. The effect of adding these nanoparticles on the mechanical behavior of the original alloy is assessed throughout tensile tests, hardness, wear and impact resistance, and relating them to the changes in the microstructure, distribution and size of nanoparticles, and the nature of the interfaces between the matrix and reinforcing material (SiC nanoparticles). Some fundamental mechanisms of solidification, hindering dislocations movement, particles reinforcing are discussed to finally determine the optimum structure that achieve the highest enhancement in mechanical properties without sacrificing the processability or plasticity required for industrial applications.

IRAQI JOURNAL OF MATERIALS
Volume (5) Issue (3) July-September 2026, pp. 133-140
Published and Sponsored by American Quality for Scientific Publishing, Inc. (AQSP)

2. Experimental Part

The chemical composition of the A356 alloy used as matrix material are listed in table (1). This alloy was selected due to its good casting capability. A mixture of SiC and aluminum particles with average particle size of 50 nm and 16 μm, respectively, was used as the reinforcement. The powders were mixed in the ratio of Al/SiC=1.67 and ball milled in isopropyl alcohol for 20 min using WC/Co balls. The mixture was then dried in a rotary vacuum evaporator and passed through a 60 mesh screen. The powder mixtures were cold pressed under 200 MPa into samples having 60×60×60 mm^3 dimension. The compacted samples were crushed and then passed through 60 mesh screen. The required amount of SiC was calculated according to the ratio of Al/SiC. Aluminum 356 alloy was selected as the matrix and 1 wt. % magnesium additive in powder form was also used as a wetting agent. Experiments were carried out using a relatively simple experimental set-up which consists of several parts as shown schematically in Fig. (1). The main part allows temperatures of up to 1000°C to be reached. This is surrounded by a 50 mm thick layer of kaowool insulator to minimize heat loss. Inside the heater band is a graphite crucible for holding the materials, which has a lid. Weighed quantity of Al-356 alloy was charged into the crucible and heated up to 750°C (above the alloy liquidus temperature) for melting. There is a nitrogen supply to the crucible in order to minimize the oxidation of molten aluminum, and a graphite stirrer mounted on a graphite shaft passes through small hole out of the crucible lid. This hole also acts as the outlet for the nitrogen gas. The shaft is connected to a digital DC motor used to stir the slurry. The end of the shaft is used to facilitate bottom pouring of the composite melt. During stirring it acts as a plug at the bottom of the crucible and, for pouring, the stirring rod assembly is lifted a distance of 5-10 mm, thus opening the stopper and allowing the slurry to flow into a mold beneath the set-up. This feature is to ensure that the impurities floating on the surface of the melt are not mixed into it. Figure (1) shows a photograph of the Al-Si alloy composite samples prepared in this work with different volumetric content of SiC nanoparticles.

Table (1) Chemical composition of the aluminum alloy used as matrix

Element	Al	Si	Fe	Cu	Mg	Mn	Zn	Ti	Ni
Wt.%	Balance	7.2	0.12	0.001	0.33	0.02	0.02	0.01	0.04

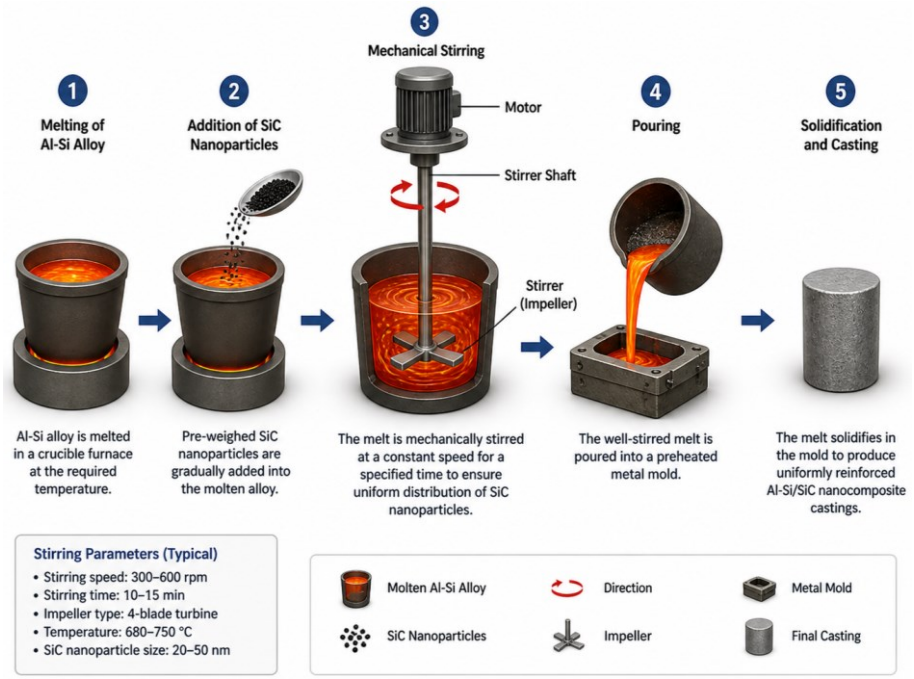

Fig. (1) Schematic explanation of the mechanical stirring casting technique used to prepare the samples in this work

IRAQI JOURNAL OF MATERIALS
Volume (5) Issue (3) July-September 2026, pp. 133-140
Published and Sponsored by American Quality for Scientific Publishing, Inc. (AQSP)

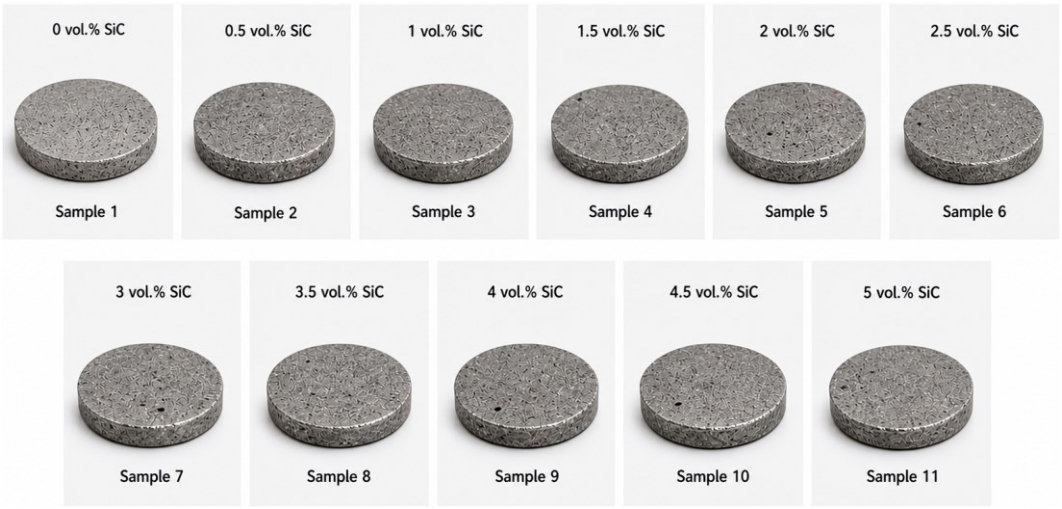

Fig. (1) The Al-Si alloy composite samples prepared in this work with different volumetric content of SiC nanoparticles

The powder mixture was inserted into an aluminum foil by forming a packet and added into molten metal of crucible when the vortex was formed. The packet of mixture melted and the particles started to distribute around the alloy sample.

Microstructural evaluations were carried out using optical microscope, scanning electron microscope (SEM) and transmission electron microscope (TEM). Optical microscope and SEM specimens were ground through grit papers and etched with Keller's reagent (2 mL HF (48%), 3 mL HCl (concentrated), 5 ml HNO_3 (concentrated) and 190 mL water). TEM specimens were machined to 0.5mm thickness and cut using a wire electro-discharge machine. The samples were then ground down (350 to 1200 grit) and perforated using double spew with methanol solution. The experimental density of the composites was obtained by the Archimedean method of weighing small pieces cut from the composite cylinder first in air and then in water, while the theoretical density was calculated using the mixture rule according to the weight fraction of the nanoparticles. The porosities of the produced composites were evaluated from the difference between the expected and the observed density of each sample.

The tension tests were used to assess the mechanical behavior of the composites. The tensile specimens were machined from composite rods according to ASTM.B 557 standard. For each volume fraction of SiC particles, three samples were tested. In order to study the effect of nanoparticles on the fracture mechanisms during tensile loading of the samples, fractography was performed on the fractured surfaces of composite specimens. To study the hardness, the Brinell hardness values of the samples were measured on the polished samples using a ball with 2.5mm diameter at a load of 31.25 kg.

3. Results and Discussion

Figure (2) shows the transmission electron microscope (TEM) and scanning electron microscope (SEM) images of the composite sample with 3.5 wt.% SiC nanoparticles. These images are crucial tools to understand the structural mechanisms responsible of the mechanical behavior of the prepared composite sample. In the TEM image, dense clusters of nanoparticles can be apparently observed with sizes ranging within 100-200 nm as these clusters appear as dark and condensed regions surrounded by aluminum-free matrix relatively empty of these particles. This inhomogeneous distribution sufficiently explains the reason of sharp decrease in the mechanical properties at volumetric percentages not exceeding 2.5 vol.%. These clusters lose their activity to hinder the Orowan strengthening because the clustered particles behave as a single large particle instead of many individually-distributed nanoparticles [23]. Also, these particles became stress-dispersion centers leading to initiate the cracks early.

When compared to Fig. (3), an observable enhancement in the distribution of the SiC nanoparticles within the matrix as they appear as individual particles or in small clusters of sizes not exceeding 50 nm with small and limited pores. This optimum distribution may cause maximum tensile resistance as the sample benefited from particle refinement (grain size of 16 μm) as well as stress strengthening mechanisms with developing structural defects (such as large pores and wide clusters) to degrade these apparently benefits. Figure (4) shows the failure mechanisms interpreting the mechanical degradation.

IRAQI JOURNAL OF MATERIALS
Volume (5) Issue (3) July-September 2026, pp. 133-140
Published and Sponsored by American Quality for Scientific Publishing, Inc. (AQSP)

In this image, the fracture section shows regions containing fine dimples referring to a limited ductile fracture, but they are widely accompanied with region of smooth facets representing a brittle fracture in addition to the presence of exposed clustered SiC nanoparticles those behave as crack-initiating sites [24,25].

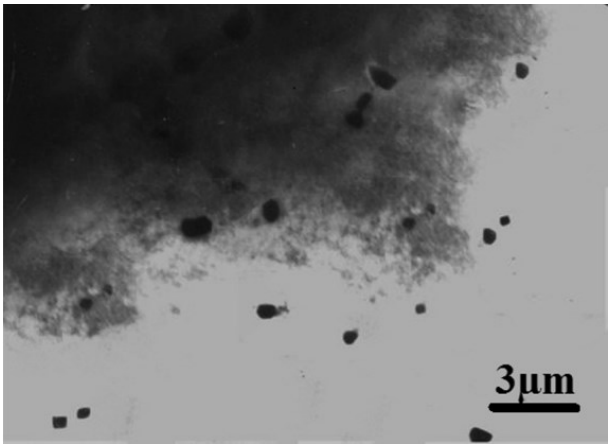

Fig. (2) TEM bright field image of composite sample with 3.5 vol.% SiC nanoparticles

Large pores with diameters up to several micrometers are clearly observed with no signs of plastic deformation around them, which confirms that these pores were already present in the sample (i.e., did not initiate during the tensile test) and acted as stress concentrators. Comparing figures (3) and (4), it is clear the sample with higher content of SiC nanoparticles sufficiently keeps good distribution and relatively low porosity to achieve the highest tensile resistance leading to convert the fracture mechanism from mostly ductile to mixed (ductile-brittle) with dominant brittle component. These microscopy results reveal undoubtedly that there is a threshold value of the volumetric percentage of nanoparticles between 2.5 and 3.5 vol.%, beyond which, the system converts from active reinforcement condition to defects-induced weakening condition despite the further addition of the reinforcing material. Consequently, the control of the manufacturing process to avoid clustering and porosity is the most crucial parameter to successfully produce composite material and not only increase the content of the nanoparticles [26].

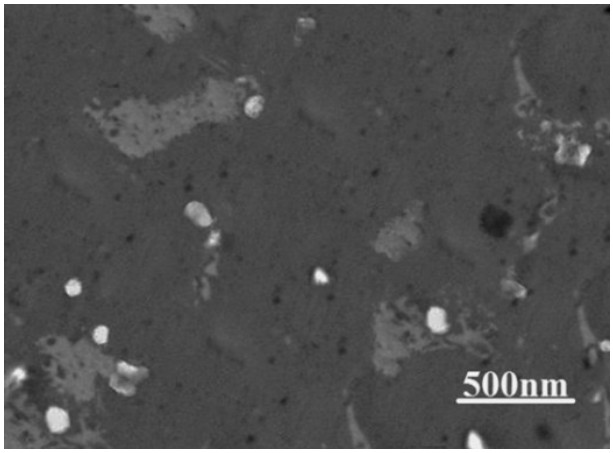

Fig. (3) SEM image of the composite sample with 3.5 vol. % SiC nanoparticles

IRAQI JOURNAL OF MATERIALS
Volume (5) Issue (3) July-September 2026, pp. 133-140
Published and Sponsored by American Quality for Scientific Publishing, Inc. (AQSP)

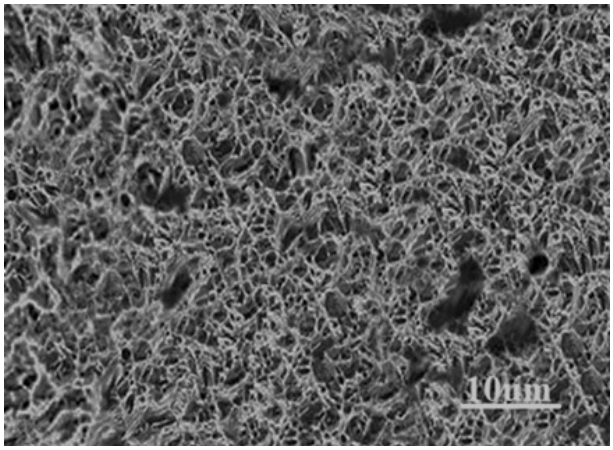

Fig. (4) SEM image of tensile fracture surface for the composites with 3.5 vol. % SiC nanoparticles

The measured values of the hardness (BHN) in Fig. (5) show an interesting nonlinear behavior, which is apparently contradicting to the conventional expectations of the typical composite materials, as the increase in hardness was rapid at the low contents of the nanoparticles, to reach its maximum at 2 vol.%, and then started to decrease despite the further increase in the content of the reinforcing material. In the fundamental unreinforced sample (0 vol.% SiC), the hardness reached 56 BHN, while after adding 0.5 vol.% SiC nanoparticles, the hardness jumped to 62 BHN with 11% increase, and to 70 BHN with 1 vol.% SiC nanoparticles. The maximum value of hardness was reached at 79 BHN with 2 vol.% SiC nanoparticles, which represents 41% enhancement with respect to the fundamental sample. This reasonable enhancement can be interpreted by two combined parameters. First, the minimum achieved grain size (16 μm) started to stabilize at 2 vol.% SiC nanoparticles, which enhances the hardness throughout the Hall-Beach mechanisms (grain refinement) [27]. Second, the porosity was relatively low (1.60%) at this content, which means that the defects were not sufficient to deactivate the effect of hardening resulted from individually distributed nanoparticles [28]. These results together refer to the existence of an optimum volumetric content of nanoparticles (2 vol.%) that maximize the hardness via the accurate balance between maximum grain refinement and minimum porosity, while the higher values lead to degrade the mechanical properties despite the existence of the reinforcing particles.

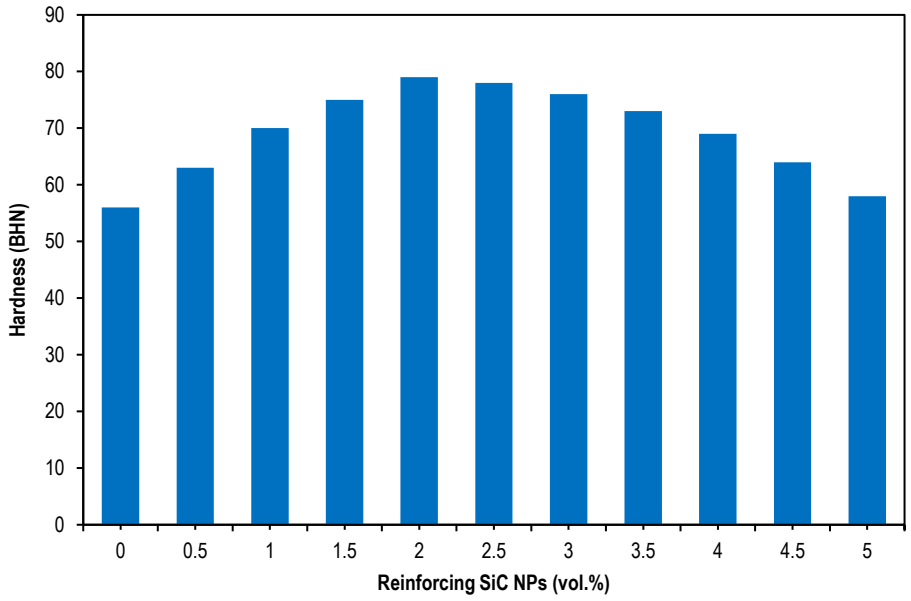

Fig. (5) Variation of hardness of the prepared composite samples with the percentage volumetric content of SiC nanoparticles in the matrix

IRAQI JOURNAL OF MATERIALS
Volume (5) Issue (3) July-September 2026, pp. 133-140
Published and Sponsored by American Quality for Scientific Publishing, Inc. (AQSP)

Figure (6) shows the variation of the yield strength of the prepared composite samples with the percentage volumetric content of SiC nanoparticles in the sample. The behavior is similar to that of the hardness a the yield strength gradually increases with SiC nanoparticles content to reach its maximum of 147 MPa at 3.5 vol.%, which is 18.3% higher than that of the fundamental sample (0 vol.% SiC). This enhancement is attributed to the same effects mentioned before in hardness section; grain refinement and Hall-Beach mechanism. As the content of reinforcing SiC nanoparticles was increased beyond 3.5 vol.%, the yield strength started to slightly decrease to reach 137 MPa at 5 vol.% SiC. This can be interpreted by the fact that the further increase in SiC nanoparticles content did not enhance the grain size (saturated at 16 µm), but, instead, caused a reasonable increase in the porosity (from 1.60% at 2 vol.% to 2.35% at 5 vol.%). The pores act as empty regions within the matrix, which reduce the effective section to hold the load as well as stress concentrators leading to initiate the early cracks and hence reduce the stress required for the permanent strain. When comparing these results with hardness results, an optimum content of the reinforcing SiC nanoparticles in the casted Al-Si alloy matrix should be determined in the range 2-3.5 vol.% to enhance the mechanical properties as an optimum balance should be achieved between different reinforcing effects (grain refinement and stress hardening) and structural defects (porosity and clusters).

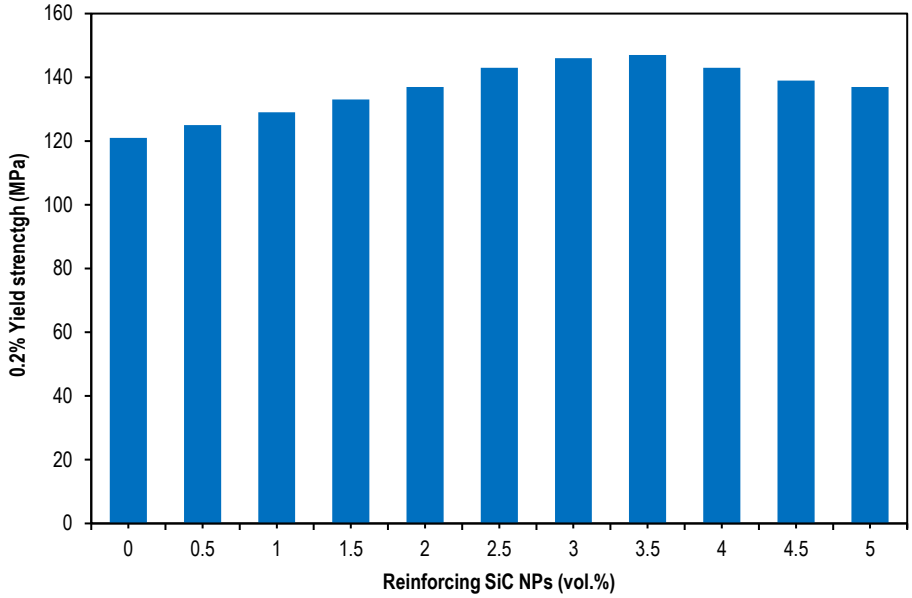

Fig. (6) Variation of 0.2% yield strength of the prepared composite samples with the percentage volumetric content of SiC nanoparticles in the matrix

Figure (7) shows the variation of the ultimate tensile strength (UTS) of the prepared composite samples with the percentage volumetric content of SiC nanoparticles in the sample. The UTS shows an interesting behavior agreeing in general with the behaviors of both hardness and yield strength as the UTS values increase with increasing the content of the reinforcing material (SiC nanoparticles) to reach a maximum of 280 MPa at 3.5 vol.% and then decrease with further increase in the of SiC nanoparticles. The maximum UTS was enhanced by 93% with respect to that of the fundamental sample (0 vol.%). Such drastic enhancement is interpreted – converse to the yield strength – by the ability of the material to elongate and plastic formation before fracture. It may benefit from slightly higher content of nanoparticles since their distribution allows additional strengthening mechanisms before the porosity becomes catastrophic. Beyond 3.5 vol.%, the UTS slightly decreased with increasing the SiC nanoparticles content to reach 247 MPa at 5 vol.%, which is 13.% lower than the maximum value of UTS. This decrease is directly related to the increasing porosity and clustering as confirmed by the TEM and SEM results as the pores and clusters represent sites for crack initiation under the effect of tensile stress. As mentioned before, this reduces the effective section to hold the maximum loading before fracture. Comparing these results to those of yield strength, the sensitivity of UTS to the increasing porosity is higher than that of the yield strength because the stage of advanced plastic deformation, and hence reaching the maximum loading, is intensively affected by the presence of microstructural defects

those accelerating the failure. Accordingly, the optimum content of the reinforcing material (SiC nanoparticles) is ranging in 2-3.5 vol.% to achieve the required balance between the mechanical properties of the casted Al-Si alloy composites.

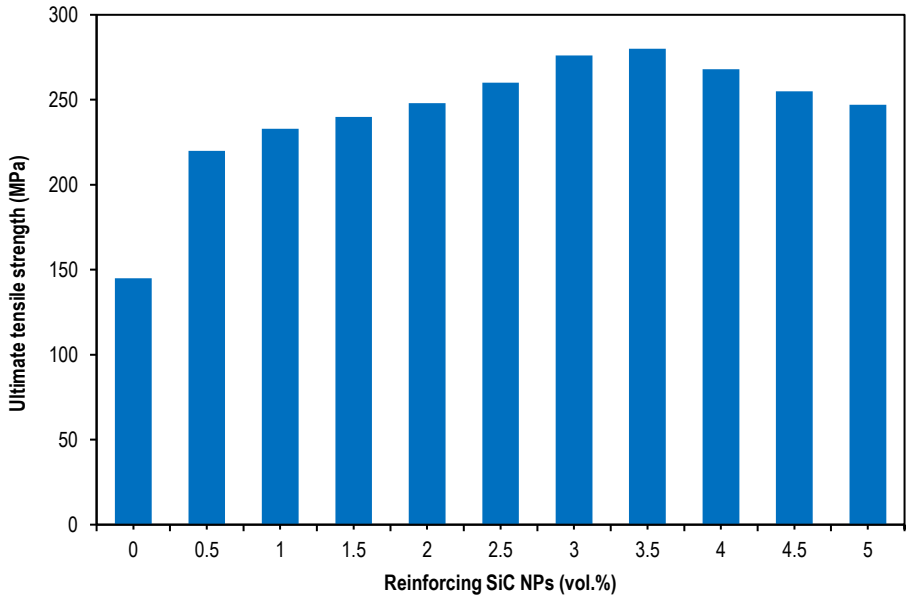

Fig. (7) Variation of the ultimate tensile strength (UTS) of the prepared composite samples with the percentage volumetric content of SiC nanoparticles in the matrix

4. Conclusion

In concluding remarks, an optimum content of the reinforcing material (SiC nanoparticles) ranging in 2-3.5 vol.% should be determined and used to achieve the best balance between reinforcing and structural defects. Increasing the content of the reinforcing material (SiC nanoparticles) beyond the optimum value leads to the formation clusters and hence increase the porosity of the sample. These clusters convert into stress centers causing early fracture and reduces the hardness and tensile strength. The mixed mode of fracture (ductile-brittle) is the dominant at the optimum content of the reinforcing material (SiC nanoparticles) with presence of fine pits and smooth surfaces indicating a shift in mechanism. The control of clusters and porosity during manufacturing process is most important than merely increasing the content of the nanoparticles as reinforcing material.

References

[1] A. Mohammadi and M. Alipour, “Effect of SiC content and milling time on the hardness and compressive strength of A380-based composites”, Mater. Today Commun., 51 (2026) 114876.
[2] K. Giridharan et al., “Investigation on the impact of tool traverse speed on the mechanical characteristics and fracture performance of friction stir welded copper CDA101 butt joints, Mater. Today Commun., 52 (2026) 115086.
[3] A.N. John, N.B.N. Jike and K.C. Nnakwo, “Evaluation of microstructure, mechanical, and tribological behavior of agro-waste hybrid reinforced high-performance Al-Si-Mg metal matrix composites”, Next Mater., 11 (2026) 101974.
[4] T. Arunkumar et al., “Development of high-performance aluminium 6061/SiC nanocomposites by ultrasonic aided rheo-squeeze casting method”, Ultrason. Sonochem., 76 (2021) 105631.
[5] S.R. Swain et al., “Tribomechanical properties of developed aluminium hybrid composites reinforced with MWCNT, SiC, and coconut shell ash”, Next Mater., 9 (2025) 101028.
[6] D. Santo et al., “Customisation of PVD coatings for biomedical devices”, Surf. Coat. Technol., 512 (2025) 132277.
[7] E.Ch. Tsirogiannis et al., “Advanced composite armor protection systems for military vehicles: Design methodology, ballistic testing, and comparison”, Compos. Sci. Technol., 251 (2024) 110486.
[8] Z. Xiao et al., “Research and development of advanced copper matrix composites”, Trans. Nonferr. Metals Soc. China, 34(12) (2024) 3789-3821.
[9] P. Bazarnik et al., “Effect of spark plasma sintering and high-pressure torsion on the microstructural and mechanical properties of a Cu–SiC composite”, Mater. Sci. Eng. A, 766 (2019) 138350.
[10] A. Lüddecke et al., “Tailoring metal powders by dry nanoparticle coating for powder bed fusion applications”, Powder Technol., 440 (2024) 119790.
[11] E.G. Zemtsova et al., “The effect of surface nanostructuring of the reinforcing phase on the mechanical properties of a nickel composite”, Procedia Struct. Integr., 65 (2024) 310-316.

[12] M.-R. Manlay et al., "Effect of a Zr source addition on the microstructure of Al-SiC composites elaborated by the Laser Powder Bed Fusion (L-PBF) process", Mater. Characteriz., 218(1) (2024) 114472.
[13] O.A. Hamadi, K.Z. Yahiya and O.N.S. Jassim, "Properties of Silicon Carbide Thin Films Deposited by Vacuum Thermal Evaporation", J. of Semicond. Technol. Sci., 5(3) (2005) 182-186.
[14] J.R. Xavier et al., "Bionanocomposites containing SnO_2 with improved chemical resistance and hydrophobic behaviours for applications in food packaging industry", Trans. Nonferr. Metals Soc. China, 33(7) (2023) 2136-2154.
[15] V.M. Rajavel Muthaiah et al., "Development of 6061AA/SiC powder metallurgy composites using microwave sintering", Next Mater., 9 (2025) 101223.
[16] O.A. Hamadi, "Characterization of SiC/Si Heterojunction Fabricated by Plasma-Induced Growth of Nanostructured Silicon Carbide Layer on Silicon Surface", Iraqi J. Appl. Phys., 12(2) (2016) 9-13.
[17] Y. Wang and P. Mertiny, "Experimental investigation for short glass fiber reinforced magnetically loaded polymer composites by compression molding on morphology and mechanical-magnetic properties", Result. Mater., 29 (2026) 100924.
[18] H.I. Akbar, E. Surojo and D. Ariawan, "Investigation of Industrial and Agro Wastes for Aluminum Matrix Composite Reinforcement", Procedia Struct. Integr., 27 (2020) 30-37.
[19] O.A. Hammadi, "Magnetically-Supported Electrically-Induced Formation of Silicon Carbide Nanostructures on Silicon Substrate for Optoelectronics Applications", Opt. Quantum Electron., 54(7) (2022) 427.
[20] Z.-y. Bian et al., "Coupling analysis on controlling mechanisms for creep of Al-Fe-Ni alloy", Trans. Nonferr. Metals Soc. China, 33(5) (2023) 1331-1344.
[21] R. Farajollahi, H. Jamshidi Aval and R. Jamaati, "Non-isothermal aging behavior of in-situ AA2024−Al3NiCu composite", Trans. Nonferr. Metals Soc. China, 32(7) (2022) 2125-2137.
[22] S.M. Ramteke et al., "Additively manufactured 316L steel reinforced by multi-layer $Ti_3C_2T_x$ for enhanced mechanical and bio-tribological performance", Surf. Coat. Technol., 511 (2025) 132321.
[23] K. Sachan, T. Narolia and R. Kumar, "Influence of microstructure in mechanical properties of light weight/high strength Al-7075 reinforced with nano and micro ZrO_2 alloy metal matrix composites", Next Mater., 11 (2026) 101892.
[24] C.-p. Yang et al., "Effect of electrolyte composition on corrosion behavior and tribological performance of plasma electrolytic oxidized TC_4 alloy", Trans. Nonferr. Metals Soc. China, 33(1) (2023) 141-156.
[25] A. Elsayed et al., "Processability and interfacial characteristics in PBF-LB/M-processed nano-B_4C/$AlSi_{10}Mg$ composites with superior high-temperature mechanical performance", Mater. Sci. Eng. A, 954 (2026) 149838.
[26] N. Anand and S.K. Selvaraj, "Ranking the wear test parameters of a hybrid ZE41 composite by means of Taguchi and Grey Relational Analysis", Next Mater., 11 (2026) 101873.
[27] L. Bharath et al., "Role of hot-rolling and heat-treatment of in-situ chemical reaction of Al7075/Gr./TiB_2 hybrid composite in microstructure, grain size and yield strength", Next Mater., 8 (2025) 100897.
[28] M.A. Shadab Siddiqui et al., "An extensive review on bibliometric analysis of carbon nanostructure reinforced composites", Result. Mater., 25 (2025) 100655.

 ISSN (print) 2958-8960 (online) 3006-6042 Printed in IRAQ